

# Experimental Observation of Non-reciprocal Waves in a Resonant Metamaterial Beam

M. A. Attarzadeh, J. Callanan, and M. Nouh\*

*Dept. of Mechanical & Aerospace Engineering, University at Buffalo (SUNY), Buffalo, New York 14260-4400*

Space-time-varying materials theoretically pledge to deliver non-reciprocal dispersion in linear systems by inducing an artificial momentum bias. Although such a paradigm eliminates the need for actual motion of the medium, experimental realization of space-time systems with dynamically changing material properties has been elusive. In this letter, we present an elastic metamaterial that exploits stiffness variations in an array of geometrically phase-shifted resonators – rather than external material stimulation – to induce a temporal modulation. We experimentally demonstrate that the resulting bias breaks time-reversal symmetry in the resonant metamaterial, and achieves a non-reciprocal tilt of dispersion modes within dynamic modulation regimes.

The ability to control wave propagation in elastic media is of key importance in a number of disciplines that span multiple geometric scales. Resonant and periodic materials aim to provide a means to mitigate or guide elastic waves via precisely engineered periodic variations in structural geometry, allowing wave control features to scale with the structure itself. Elastic vibrations of solids have been well studied and characterized [1–3], however the field of elastic metamaterials possessing unique dispersive features including tunable band gaps, topological edge states, and negative effective properties has received increased attention in recent years [4–7]. Most recently, novel configurations have been presented as pathways to break one of the fundamental elastodynamic principles, *reciprocity*, and onset a diode-like behavior [8, 9], as well as logical gates in mechanical systems [10]. Reciprocity, often used in conjunction with principles of superposition and symmetry, is of key importance for many analysis methods in electromagnetism, acoustics, and signal processing – in practice, however, back scattered waves present a number of issues and limitations in sensing, structural fidelity, telecommunication and defense applications. Therefore, it is of key interest to develop structures that exhibit a robust non-reciprocal wave propagation behavior. Systems with space-time modulated material fields have been the focus of a number of efforts to investigate wave amplification and non-reciprocity in linear systems [11, 12]. Due to the time dependence of their properties, these materials are no longer bound by the reciprocity, while, unlike nonlinear systems, their response remains amplitude-independent [13]. The theoretical problem of characterizing elastic wave propagation in space-time modulated structures has been investigated in one- [14] and two-dimensional [15] systems using plane wave expansion. Recently, this approach has been further extended to discretely modulated structures [16] to better adapt with practical situations. Non-reciprocal waves have also been witnessed in locally resonant systems [17, 18] and elastic metamaterial beams [19]. Nonetheless, the realization of time modulated elastic systems remains a practical challenge due to their dynamic nature.

A select number of efforts have conceived ways to realize non-reciprocal media. This includes – but is not limited to – using photo-elastic effects [6], magneto-elastic effects [20–23], piezoelectric materials [24–26], geometric non-linearity [27, 28], or using gyroscopic effects via angular momentum modulations [29]. The band gap tunability observed in granular materials with dielectric properties [30, 31] are also promising in providing realizable avenues to break reciprocity.

In this work, we present a novel apparatus that achieves space-time modulation of elastic stiffness in a magnet-free configuration that does not involve smart or adaptive materials with inter-physical couplings. The system, which is designed and constructed using widely available components and manufacturing techniques, comprises a sub-wavelength elastic metamaterial beam (or metabeam, for short) and relies on local resonators that dynamically vary their effective stiffness by changing their angular orientation with respect to the vibration direction, owing to their geometric design. As such, a prescribed phase shift between the resonators is used to generate a spatial modulation of the beam’s stiffness, in conjunction with synchronized rotations of the resonator array to induce a wave-like space-time stiffness variation along the length of the metabeam. In addition to the breakage of wave propagation symmetry, the proposed design inherits the tunability of frequency band gaps in conventional metamaterials, which in turn extends the non-reciprocal behavior to low frequencies. Following the introduction, the operational principles are outlined in detail; next, a description of the apparatus is given, and finally dispersion patterns are experimentally constructed via laser Doppler vibrometry, ultimately demonstrating and verifying the non-reciprocal energy transmission in the metamaterials medium.

*Operational Principle*— The non-reciprocal metabeam is conceptually similar to a locally resonant flexural metamaterial depicted in Fig. 1a and its well-established dynamics [32, 33]. The metabeam consists of a series of mechanical spring-mass resonators connected to a host beam. The spring stiffness in each resonator, however, is varied independently in time, and by controlling the macroscopic spatial distribution of the resonators’ stiffness, a specific space-time traveling profile is achieved.

\* Corresponding author: mnouh@buffalo.edu

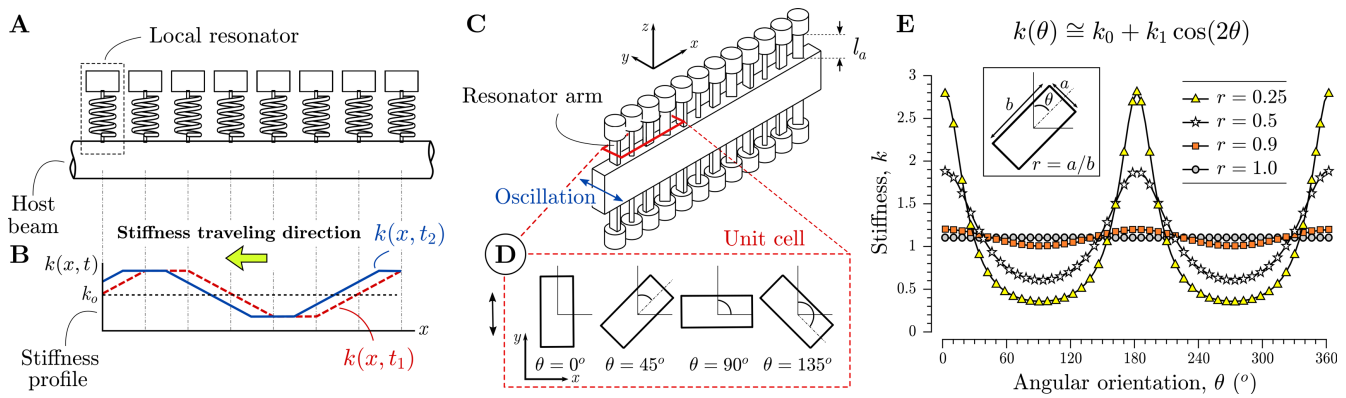


FIG. 1. Schematic representation of the operational principles of the non-reciprocal metabeam: A. Illustration of a conventional metabeam with discretely located resonators; B. Space-time variation of resonators' stiffness traveling in the negative direction of the  $x$ -axis to induce artificial linear momentum bias; C. Proposed realization of the spatially modulated resonator stiffness in an elastic metabeam; D. Angular orientation of resonators in a unit-cell to create the spatial modulation; E. The stiffness variation of rectangular cross sections with various aspect ratios versus angular orientation.

Fig. 1b shows an example of the effective stiffness variation necessary to create a non-reciprocal metabeam. The stiffness  $k(x, t)$  is graphed for two time instants,  $t_1$  and  $t_2$ . The curve  $k(x, t_2)$  is identical to  $k(x, t_1)$  except for a spatial phase shift, i.e. the stiffness profile varies like a wave traveling along the structure to simulate an artificial linear momentum bias leading to non-reciprocal wave dispersion [34]. The means of achieving this stiffness variation, however, are of paramount importance for both research and practical implementation purposes. We propose that, rather than employ a smart material which directly varies its properties when interacting with an external field [20] – as such materials are only practical within a limited physical scale and often prohibitively expensive in addition to being uncommon – the stiffness variation can be enforced by making use of the basic properties of a beam in bending: the second area moment. Considering a simple beam as the spring member (hereafter referred to as resonator arm, or arm to distinguish from the host beam) with rectangular cross section, as shown in Fig. 1c, the lateral stiffness under Euler-Bernoulli theory is given by  $k = 3EI_x/l_a^3$ , where  $E$  is the elastic modulus,  $l_a$  is the arm length, and  $I_x$  is second area moment of arm cross section calculated perpendicular to the vibration direction. Modifying the elastic modulus  $E$  in order to achieve effective and instantaneous control over the resonator stiffness has been the subject of many research efforts, however doing so requires materials with multi-physics coupling which introduces various layers of complexity. In this work, instead, we take a different route and control the second area moment – which is dependant on the orientation of the arm with respect to the vibration direction – to periodically change the resonator stiffness in a scalable, yet effective way. As per Fig. 1d, the relevant second area moment is

$$I_x = \int_A y^2 dA \quad (1)$$

The stiffness can be computed for each resonator according to Eq. 1, or, alternatively, using the principle axes values and coordinate transformation by an angle  $\theta$ . Let  $x'$  and  $y'$  be the principle axes for one resonator arm; the relevant moment of area for vibration in the  $y$  direction as depicted in Fig. 1c is

$$I_x = I_0 + I_1 \cos(2\theta) \quad (2)$$

where  $I_0 = \frac{1}{2}(I_{x'} + I_{y'})$  and  $I_1 = \frac{1}{2}(I_{x'} - I_{y'})$ . We observe that the difference in magnitude between the two principle moments determines the alternating variation of  $I_x$  and in turn the variation in the resonator stiffness. A series of finite element numerical simulations were carried out to verify the change in stiffness as a result of the resonator angular rotation. Fig. 1e shows the stiffness variation with respect to the rotation angle for rectangular cross sections with aspect ratios  $r = 0.25, 0.5, 0.9$  and  $1$ . Fig. 1e confirms that a lower aspect ratio between the two sides in the rectangular cross section results in a greater variation in the arm stiffness as it rotates. Nonetheless, the stiffness variation starts deviating from a perfect harmonic variation due to violation of Euler-Bernoulli beam assumptions. Fig. 1d shows the angular orientation of the resonators in one unit cell in a metabeam with spatially modulated resonator stiffness. The orientation of each adjacent resonator is rotated by  $45^\circ$  relative to the previous one such that a repeating unit cell is made up of four local resonators. The effectiveness of the orientation-dependent stiffness is demonstrated by operating the metamaterial in two static regimes, as depicted in Fig. 2. The shown dispersion as well as response characteristics confirm that energy transmission in metabeam can be dramatically altered only by changing orientation of all resonators by  $90$  degrees to switch from the lowest to the highest stiffness configurations (a band gap shift of nearly  $400$  Hz).

The host beam in Fig. 1c is equipped with a series of local resonators that consist of a prismatic resonator arm

and a tip mass. Let the index  $j$  denote a single resonator (more specifically a pair of resonators at the same  $x$  location on the beam, top and bottom); a unit cell on the metabeam consists of  $J$  resonator pairs. The space-time modulation of the resonators' stiffness is achieved by rotating the resonators' arms with an angular velocity of  $\omega_p$  (temporal modulation) while maintaining the aforementioned spatial modulation ( $45^\circ$  phase shift between angular orientation of adjacent unit cells). The combined effect of both spatial and temporal variation creates the desired traveling-wave variation of resonators' stiffness. As such, stiffness of the  $j^{\text{th}}$  resonator at time  $t$  is

$$k^{(j)}(t) = k_0 + k_1 \cos(\omega_p t + \phi_j) \quad (3)$$

where,  $\phi_j = \pi j/J$ . Note that the stiffness profile changes in both space and time along the length of the beam and follows a traveling wave-like profile. The development of the space-time modulated resonator stiffness has been motivated by recent literature until this point. We have outlined a novel method for realizing a traveling stiffness wave which does not rely on exotic or expensive materials and is achieved by simply varying the resonator geometry with respect to the vibration direction. In the following sections we will experimentally demonstrate the effectiveness of this approach.

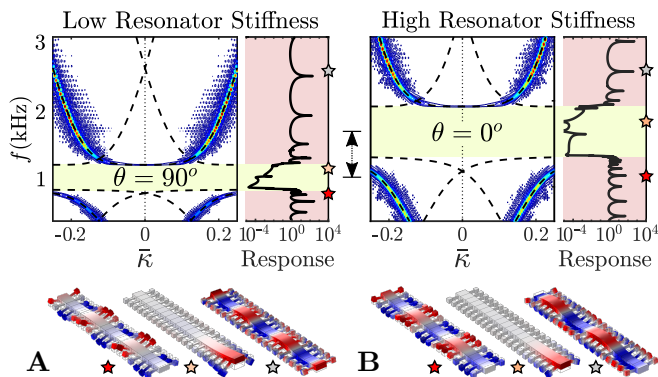


FIG. 2. Dispersion behavior and transmission spectra of the metabeam in two static configurations: A. Low stiffness ( $\theta = 90^\circ$ ) and B. High stiffness ( $\theta = 0^\circ$ ). Shaded regions indicate band gap frequencies. Mode shapes pre, within, and post both band gaps are provided for reference.

*Experimental Apparatus*— The metabeam was constructed following the general operating principles as shown in Fig. 1. The setup consists of the host beam, forty local resonators grouped into symmetric pairs above and below the beam, and motors to control the resonator angle. A solid ABS plastic beam was CNC-machined to a length of 48 in., width of 1.50 in., and height of 2.875 in. A series of 40 pockets were cut out from the beam to house NEMA 8 bipolar stepper motors. The resonator arms were machined from 6061 aluminum to a height of 2.0 in., width of 0.625 in., and thickness of 0.280 in. The tip masses were machined from low carbon steel to a diameter of 1.375 in. and a height of 1.0 in. The resonators

were each individually adjusted to within 0.010 in. of concentricity (runout) between the motor shaft and the tip mass outer diameter to minimize vibrations induced into the structure when the arms were rotating. The stepper motors were driven with a custom driver array using widely available microstepping breakout boards. In a typical test the motors were commanded to accelerate slowly to a speed of 2000 RPM (33.3 Hz) and, after maintaining this speed for 10 minutes, commanded to decelerate to a stop: throughout one such maneuver the motors received 3,731,600 step commands and were observed to return to their original position to within an average error of less than one step (*see supplementary material*).

Maintaining a constant host structure temperature throughout the test runs was a challenge due to the motors being confined within the host structure. It was found that with sufficient convection cooling the structure would maintain a steady-state temperature. Fig. 3 shows an illustration of the elastic metabeam and test equipment system. The metabeam is represented by a black rectangle with the local resonators as circles, similar to a bird's eye view of the actual apparatus. Vibration measurements were taken with a Polytec PSV-500 Scanning Laser Doppler Vibrometer (SLDV). The temperature of the beam was continuously monitored with a FLIR A325sc thermal imaging camera to ensure that the stiffness of the host structure did not vary due to heating or cooling. Actuators in the form of two extender piezoelectric plates (and a high voltage amplifier) were mounted symmetrically on both sides of the beam and actuated  $180$  degrees out of phase such that transverse vibrations are dominantly excited. The motors and piezoelectric actuators were directly controlled using LabVIEW and an NI DAQ along with the custom motor driver array. Further, the SLDV system was triggered using the LabVIEW in order to ensure measurements synchronous with prescribed temporal modulation of the metabeam. In a time-invariant system, an SLDV triggers the excitation and controls the measurement to ensure that the final results can be used to reconstruct a coherent data set. With a time-periodic structure, however, the SLDV must be triggered by an external controller to make certain that the measurements at each spatial point are taken at the same phase with respect to the system's time variation. The LabVIEW controller was used to trigger the vibrometer on a specified integer number of resonator rotations such that each measurement at a given point in space started with the motors at the same orientation, regardless of their rotational velocity. A close-up view of one super cell in the metabeam is shown in Fig. 3e revealing the angular phase shifts within one cycle. The time domain signal that is sent to the high voltage amplifier is a wide-band tone burst excitation with a central frequency of 1500 Hz.

*Results*— The SLDV system acquires time-domain data by repeatedly exciting the system with the same signal and taking measurements at different locations along the length of the beam. The post-processing of

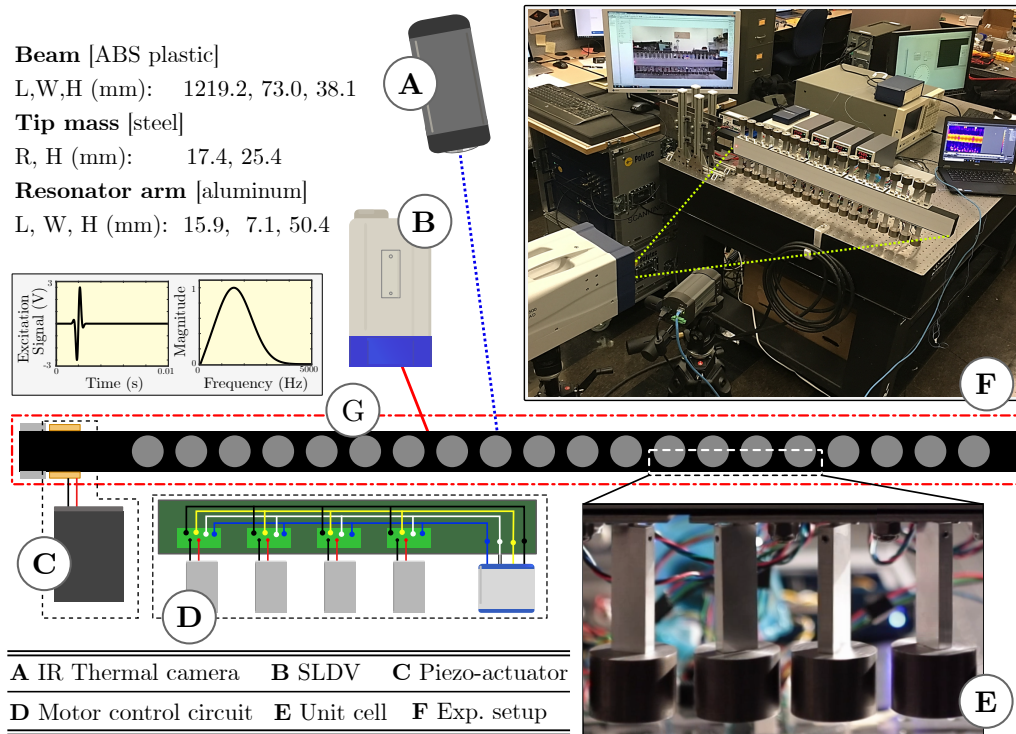


FIG. 3. Illustration of the complete experimental apparatus for the non-reciprocal elastic metabeam: A. Thermal imaging camera; B. Scanning Laser Doppler Vibrometer (SLDV) imaging system; C. Beam excitation module and the signal sent to the piezoelectric actuator; D. Power and controller circuit; E. Unit cell (bottom half, close-up); F. and G. Metabeam

the data is carried out in the numerical computing package, MATLAB. After exporting the captured displacement field for every time step from the vibrometer acquisition software, spatial and temporal Fourier transformations are performed to extract the frequency content of propagating waves. The result is then normalized by the excitation spectrum. By adopting a cantilever beam configuration with the ability to reverse the motor direction, we can effectively double the length of the beam without increasing the size of the structure: waves traveling from the piezoelectric actuator while the motors are rotating clockwise (CW) can be treated as waves traveling in the opposite direction within the structure while the motors are rotating counter-clockwise (CCW). As such, we can perform two tests on a cantilever beam of roughly 1 m length, one with CW rotation and one with CCW rotation, effectively mimicking a single test on a beam of length 2 m with a central excitation. Making use of this strategy, the manufactured metabeam was tested at two different modulation regimes, *quasi-static* and *dynamic*, based on the rotational speed of the motors.

In the quasi-static modulation regime, the motors are rotated at a relatively low speed, 100 RPM (1.67 Hz), compared to the natural frequencies of the resonators – which are higher than 1000 Hz. In addition, the resonators are oriented in a way to mimic a spatially periodic variation of stiffness along the structure (similar to what is shown in Fig. 1c). The combination of the spa-

tial phase shift and the low-speed motor rotation generates space-time modulation of stiffness that slowly creeps along the metabeam. With a CCW direction command, a forward modulation appears that is moving from root to the end of the beam; while, a CW command results in a backward modulation with stiffness moving in the opposite direction. This slow variation of stiffness is reminiscent of adiabatic pumping in quantum mechanical systems [35, 36]. Despite the proven unconventional topological aspects of such systems [17, 37], here we limit our attention to the spectral properties of the metabeam and dispersion characteristics rather than topological features of the modes. The metabeam is tested in both clockwise and counter-clockwise rotations at 100 RPM and Fig. 4a illustrates the experimentally retrieved dispersion and transmission of the metabeam within the frequency range of interest, 600 to 3000 Hz. The right half-plane of the dispersion contours corresponds to the forward modulation and the left half-plane corresponds to the backward modulation, which are shown along with their respective transmissions in Fig. 4a. Note that the repeated flat lines in the dispersion plots (and alternating peaks in the spectra) are artifacts of the stepping frequency of the stepper motors that occurs at 200 times the rotational frequency (or 333.3 Hz); they are kept in the results to maintain originality and reproducibility of the data. Due to the reciprocal nature, they do not interfere with our interpretation of the results. From the zoomed

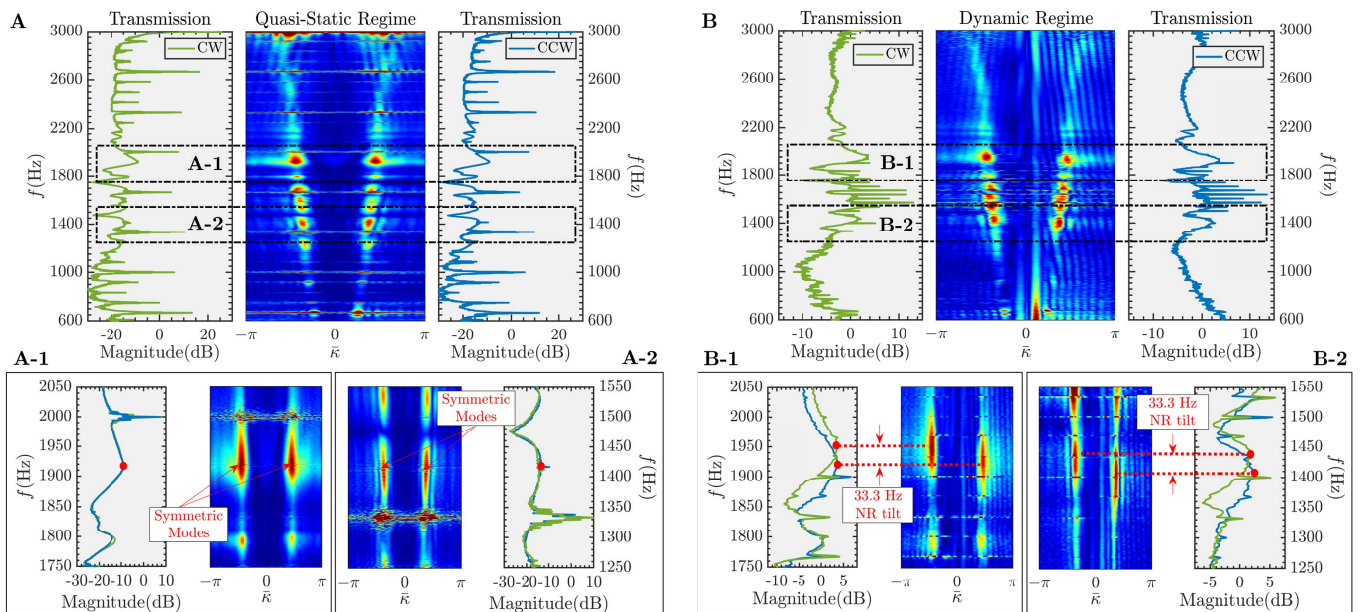


FIG. 4. Experimental results: A. Quasi-Static modulation regime with motors rotating at 100 rpm (1.67 Hz). Experimentally reconstructed dispersion patterns and transmission spectra obtained from forward (CCW rotation) and backward (CW rotation) modulated structures showing reciprocal response with fairly symmetrical counter-propagating modes due to low speed modulation (A-1. Close-up: 1750 – 2050 Hz. A-2. Close-up: 1250 – 1550 Hz). B. Dynamic modulation regime with motors rotating at 2000 rpm (33.3 Hz). Experimentally reconstructed dispersion patterns and transmission spectra obtained from forward (CCW) and backward (CW) modulated structures showing non-reciprocal tilt equal to the exact amount of the motors’ rotational speed for counter-propagating mode (B-1. Close-up: 1750 – 2050 Hz. B-2. Close-up: 1250 – 1550 Hz).

view in Figs. 4a-1 and 4a-2 we conclude that insignificant non-reciprocity between the forward and backward dispersion modes exists for this case. As intended, the traveling speed of the modulation (or the speed of motors) in the quasi-static modulation regime is insufficient to instigate detectable non-reciprocal response regardless of the rotational direction of the motors.

In the dynamic modulation regime, we intentionally increase the rotational speed of the motors to 2000 RPM (33.3 Hz) – while maintaining the spatial modulation (angular position phase shift between the successive resonators). The result is a much faster traveling modulation and is shown in Fig. 4b along with the transmission spectra for both forward and backward modulations. As observed from the zoomed view in Figs. 4b-1 and 4b-2, the faster modulation speed in the dynamic regime generated one-way modal transition and detectable non-reciprocal tilt of the dispersion modes. As a result, the rightward propagating branch is downshifted by the amount of 33.3 Hz (equal to the modulation speed, or rotational speed of motors) compared to the left propagating branch, which indicates the effectiveness of the proposed metabeam to break time-reversal symmetry. In accordance with the previous findings on reciprocity breakage in space-time modulated systems: the frequency shift between the forward and the backward propagating branches is an integer multiple of the modulation frequency [37, 38]. Accordingly, the non-

reciprocity can be further accentuated by increasing the rotational speed of the motors. Importantly, the one way transmission at a given frequency can also be switched in the opposite direction by simply rotating motors in the opposite direction.

*Conclusion*— This work introduced a first experimental realization of dynamically modulated metamaterials that do not rely on material response to external stimulus, but rather an inherent geometric feature by design. A cornerstone feature of flexural materials, second area moment, was used to geometrically induce a space-time modulation and, consequently, enforce an artificial linear momentum bias to break time-reversal symmetry of waves in an elastic beam. It was experimentally demonstrated that non-reciprocal tilt of the dispersion modes is directly correlated with the modulation speed of the medium and can be adjusted all the way from complete reciprocal dispersion in the quasi-static regime to a complete non-reciprocal dispersion in the dynamic modulation regime. Further, the current design also shows great potential to harbor topologically interesting features in future efforts. For instance, the quasi-static mode allows for adiabatic evolution of eigen-structure which provides a realizable route to create topologically protected boundary modes in elastic structures.

The work was supported by the US National Science Foundation through Award no. 1847254 (CAREER) as well as the Vibration Institute through the Academic Grant program.

- [1] J. F. Doyle, Wave propagation in structures, in *Wave Propagation in Structures* (Springer, 1989) pp. 126–156.
- [2] D. Mead, Wave propagation in continuous periodic structures: research contributions from southampton, 1964–1995, *Journal of sound and vibration* **190**, 495 (1996).
- [3] M. I. Hussein, M. J. Leamy, and M. Ruzzene, Dynamics of Phononic Materials and Structures: Historical Origins, Recent Progress, and Future Outlook, *Applied Mechanics Reviews* **66**, 040802 (2014).
- [4] P. Celli and S. Gonella, Tunable directivity in metamaterials with reconfigurable cell symmetry, *Applied Physics Letters* **106**, 10.1063/1.4914011 (2015).
- [5] Y. Chen, G. Huang, and C. Sun, Band gap control in an active elastic metamaterial with negative capacitance piezoelectric shunting, *Journal of Vibration and Acoustics* **136**, 061008 (2014).
- [6] N. Swintek, S. Matsuo, K. Runge, J. Vasseur, P. Lucas, and P. Deymier, Bulk elastic waves with unidirectional backscattering-immune topological states in a time-dependent superlattice, *Journal of Applied Physics* **118**, 063103 (2015).
- [7] H. H. Huang, C. T. Sun, and G. L. Huang, On the negative effective mass density in acoustic metamaterials, *International Journal of Engineering Science* **47**, 610 (2009).
- [8] M. B. Zanjani, A. R. Davoyan, A. M. Mahmoud, N. Engheta, and J. R. Lukes, One-way phonon isolation in acoustic waveguides, *Applied Physics Letters* **104**, 081905 (2014).
- [9] R. Fleury, D. L. Sounas, C. F. Sieck, M. R. Haberman, and A. Alù, Sound isolation and giant linear nonreciprocity in a compact acoustic circulator, *Science* **343**, 516 (2014).
- [10] O. R. Bilal, A. Foehr, and C. Daraio, Bistable metamaterial for switching and cascading elastic vibrations, *Proceedings of the National Academy of Sciences* **114**, 4603 (2017).
- [11] A. Cullen, A travelling-wave parametric amplifier, *Nature* **181**, 332 (1958).
- [12] E. Cassidy and A. Oliner, Dispersion relations in time-space periodic media: Part i, stable interactions, *Proceedings of the IEEE* **51**, 1342 (1963).
- [13] J. Achenbach, *Wave propagation in elastic solids*, Vol. 16 (Elsevier, 2012).
- [14] G. Trainiti and M. Ruzzene, Non-reciprocal elastic wave propagation in spatiotemporal periodic structures, *New Journal of Physics* **18**, 083047 (2016).
- [15] M. Attarzadeh and M. Nouh, Non-reciprocal elastic wave propagation in 2d phononic membranes with spatiotemporally varying material properties, *Journal of Sound and Vibration* **422**, 264 (2018).
- [16] E. Riva, J. Marconi, G. Cazzulani, and F. Braghin, Generalized plane wave expansion method for non-reciprocal discretely modulated waveguides, *Journal of Sound and Vibration* **449**, 172 (2019).
- [17] M. Attarzadeh, H. Al Ba'ba'a, and M. Nouh, On the wave dispersion and non-reciprocal power flow in space-time traveling acoustic metamaterials, *Applied Acoustics* **133**, 210 (2018).
- [18] H. Nassar, H. Chen, A. Norris, M. Haberman, and G. Huang, Non-reciprocal wave propagation in modulated elastic metamaterials, in *Proc. R. Soc. A*, Vol. 473 (The Royal Society, 2017) p. 20170188.
- [19] H. Nassar, H. Chen, A. Norris, and G. Huang, Non-reciprocal flexural wave propagation in a modulated metabeam, *Extreme Mechanics Letters* **15**, 97 (2017).
- [20] M. Ansari, M. Attarzadeh, M. Nouh, and M. A. Karami, Application of magnetoelastic materials in spatiotemporally modulated phononic crystals for nonreciprocal wave propagation, *Smart Materials and Structures* **27**, 015030 (2017).
- [21] A. Nanda and M. A. Karami, One-way sound propagation via spatio-temporal modulation of magnetorheological fluid, *The Journal of the Acoustical Society of America* **144**, 412 (2018).
- [22] Y. Wang, B. Yousefzadeh, H. Chen, H. Nassar, G. Huang, and C. Daraio, Observation of non-reciprocal wave propagation in a dynamic phononic lattice, *Physical review letters* **121**, 194301 (2018).
- [23] Y. Chen, X. Li, H. Nassar, A. N. Norris, C. Daraio, and G. Huang, Nonreciprocal wave propagation in a continuum-based metamaterial with space-time modulated resonators, *Physical Review Applied* **11**, 064052 (2019).
- [24] C. Croëne, J. Vasseur, O. Bou Matar, M.-F. Ponge, P. Deymier, A.-C. Hladky-Hennion, and B. Dubus, Brillouin scattering-like effect and non-reciprocal propagation of elastic waves due to spatio-temporal modulation of electrical boundary conditions in piezoelectric media, *Applied Physics Letters* **110**, 061901 (2017).
- [25] G. Trainiti, Y. Xia, J. Marconi, G. Cazzulani, A. Erturk, and M. Ruzzene, Time-periodic stiffness modulation in elastic metamaterials for selective wave filtering: Theory and experiment, *Physical review letters* **122**, 124301 (2019).
- [26] J. Marconi, E. Riva, M. Di Ronco, G. Cazzulani, F. Braghin, and M. Ruzzene, Experimental observation of non-reciprocal band-gaps in a space-time modulated beam using a shunted piezoelectric array, *arXiv preprint arXiv:1909.13224* (2019).
- [27] S. P. Wallen and M. R. Haberman, Nonreciprocal wave phenomena in spring-mass chains with effective stiffness modulation induced by geometric nonlinearity, *Physical Review E* **99**, 013001 (2019).
- [28] B. M. Goldsberry, S. P. Wallen, and M. R. Haberman, Non-reciprocal wave propagation in mechanically-modulated continuous elastic metamaterials, *The Journal of the Acoustical Society of America* **146**, 782 (2019).
- [29] M. A. Attarzadeh, S. Maleki, J. L. Crassidis, and M. Nouh, Non-reciprocal wave phenomena in energy self-reliant gyric metamaterials, *The Journal of the Acoustical Society of America* **146**, 789 (2019), <https://doi.org/10.1121/1.5114916>.
- [30] N. NejadSadeghi, L. Placidi, M. Romeo, and A. Misra, Frequency band gaps in dielectric granular metamaterials modulated by electric field, *Mechanics Research Communications* **95**, 96 (2019).
- [31] N. NejadSadeghi and A. Misra, Axially moving materials with granular microstructure, *International Journal of Mechanical Sciences* **161**, 105042 (2019).
- [32] H. Sun, X. Du, and P. F. Pai, Theory of metamaterial beams for broadband vibration absorption, *Journal of In-*

- telligent Material Systems and Structures (2010).
- [33] H. B. Al Ba'ba'a and M. Nouh, Mechanics of longitudinal and flexural locally resonant elastic metamaterials using a structural power flow approach, *International Journal of Mechanical Sciences* **122**, 341 (2017).
  - [34] M. Attarzadeh and M. Nouh, Elastic wave propagation in moving phononic crystals and correlations with stationary spatiotemporally modulated systems, *AIP Advances* **8**, 105302 (2018).
  - [35] Y. E. Kraus, Y. Lahini, Z. Ringel, M. Verbin, and O. Zeitlinger, Topological states and adiabatic pumping in quasicrystals, *Physical review letters* **109**, 106402 (2012).
  - [36] L. Wang, M. Troyer, and X. Dai, Topological charge pumping in a one-dimensional optical lattice, *Physical review letters* **111**, 026802 (2013).
  - [37] R. Chaunsali, F. Li, and J. Yang, Stress wave isolation by purely mechanical topological phononic crystals, *Scientific reports* **6**, 30662 (2016).
  - [38] H. Nassar, H. Chen, A. Norris, and G. Huang, Quantization of band tilting in modulated phononic crystals, *Physical Review B* **97**, 014305 (2018).